The Folylpolyglutamate Synthetase Plastidial Isoform Is Required for Postembryonic Root Development in Arabidopsis[1][W][OA]

Avinash C. Srivastava, Perla A. Ramos-Parra, Mohamed Bedair, Ana L. Robledo-Hernández, Yuhong Tang, Lloyd W. Sumner, Rocío I. Díaz de la Garza, and Elison B. Blancaflor*

Plant Biology Division, Samuel Roberts Noble Foundation, Ardmore, Oklahoma 73401 (A.C.S., M.B., Y.T., L.W.S., E.B.B.); Departamento de Agrobiotecnología y Agronegocios, División de Biotecnología e Ingeniería de Alimentos, Tecnológico de Monterrey, Monterrey, Nuevo Leon 64849, Mexico (P.A.R.-P., A.L.R.-H, R.I.D.d.l.G.); and BioEnergy Science Center, United States Department of Energy, Oak Ridge, Tennessee 37831 (A.C.S., Y.T., E.B.B.)

A recessive Arabidopsis (*Arabidopsis thaliana*) mutant with short primary roots and root hairs was identified from a forward genetic screen. The disrupted gene in the mutant encoded the plastidial isoform of folylpolyglutamate synthetase (FPGS), previously designated as AtDFB, an enzyme that catalyzes the addition of glutamate residues to the folate molecule to form folylpolyglutamates. The short primary root of *atdfb* was associated with a disorganized quiescent center, dissipated auxin gradient in the root cap, bundled actin cytoskeleton, and reduced cell division and expansion. The accumulation of monoglutamylated forms of some folate classes in *atdfb* was consistent with impaired FPGS function. The observed cellular defects in roots of *atdfb* underscore the essential role of folylpolyglutamates in the highly compartmentalized one-carbon transfer reactions (C1 metabolism) that lead to the biosynthesis of compounds required for metabolically active cells found in the growing root apex. Indeed, metabolic profiling uncovered a depletion of several amino acids and nucleotides in *atdfb* indicative of broad alterations in metabolism. Methionine and purines, which are synthesized de novo in plastids via C1 enzymatic reactions, were particularly depleted. The root growth and quiescent center defects of *atdfb* were rescued by exogenous application of 5-formyl-tetrahydrofolate, a stable folate that was readily converted to metabolically active folates. Collectively, our results indicate that AtDFB is the predominant FPGS isoform that generates polyglutamylated folate cofactors to support C1 metabolism required for meristem maintenance and cell expansion during postembryonic root development in Arabidopsis.

The growth and development of a root is dictated by the coordinated activity of cell division, cell expansion, and cell differentiation. Forward genetic screens for root mutants in the model plant Arabidopsis (*Arabidopsis thaliana*) have uncovered complex developmental networks that orchestrate patterns of cell division in the meristem and trigger the onset or extent of longitudinal cell expansion in the elongation zone. Mutant studies also have led to the discovery of signaling pathways that specify the position of root hair emergence, which typically accompany the maturation of cells in the zone of differentiation or define the polarity of root hair growth (Benfey et al., 2010). Components of these signaling and developmental networks include a dynamic cytoskeleton and vesicular trafficking system, both of which play pivotal roles in regulating membrane recycling and cell wall deposition to sustain normal root growth (Bernal et al., 2008; Yoo et al., 2008; Beck et al., 2010). Also part of the intricate developmental networks that govern root growth are a collection of transcription factors and an array of chemical messengers, including sugars, nutrients, amino acids, and most of the major plant hormones (Benková and Hejátko, 2009; Forde and Walch-Liu, 2009; Iyer-Pascuzzi et al., 2009).

Although plant hormones continue to dominate studies of chemical signals that regulate root development, there is accumulating evidence for the involvement of other endogenous metabolites such as vitamins in the maintenance of normal root morphology. For example, pyridoxine (vitamin B6) has been linked to the control of Arabidopsis root growth since a mutant in a gene that encodes a pyridoxine synthase

[1] This work was supported by the Samuel Roberts Noble Foundation, the Oklahoma Center for the Advancement of Science and Technology (grant no. PSB10–004 to E.B.B.), the BioEnergy Science Center (to Y.T. and E.B.B.), and the Mexican National Council for Research and Technology (grant no. 80459 to R.I.D.d.l.G.). The BioEnergy Science Center is a U.S. Department of Energy Bioenergy Research Center supported by the Office of Biological and Environmental Research in the Office of Science, U.S. Department of Energy.

* Corresponding author; e-mail eblancaflor@noble.org.

The author responsible for distribution of materials integral to the findings presented in this article in accordance with the policy described in the Instructions for Authors (www.plantphysiol.org) is: Elison B. Blancaflor (eblancaflor@noble.org).

[W] The online version of this article contains Web-only data.

[OA] Open Access articles can be viewed online without a subscription.

www.plantphysiol.org/cgi/doi/10.1104/pp.110.168278

1 (*pdx1*) exhibited shorter primary roots compared with the wild type (Chen and Xiong, 2005; Wagner et al., 2006). In addition to their protective roles against oxidative stress, vitamins serve as cofactors for several enzymes that metabolize compounds required for normal cellular function. Thus, the root growth defects reported in Arabidopsis *pdx1* could be the result of alterations in metabolic pathways that are critical for the biosynthesis of compounds required for normal cell physiology. For example, the stunted root development in *pdx1* was associated with impaired local auxin biosynthesis and a broad disruption in metabolism that led to altered levels of amino acids, sugars, and various organic acids (Wagner et al., 2006; Chen and Xiong, 2009).

Tetrahydrofolate (THF) and its derivatives, collectively referred to as folates, constitute a group of B vitamins (vitamin B9) that are essential for several major metabolic pathways in the cell because they mediate the addition and removal of one-carbon (C1) units in a set of reactions commonly referred to as C1 metabolism. The products of these C1 transfer reactions include purines, Met, thymidylate, and pantothenate (vitamin B5), all of which are crucial for the normal function of living cells (Hanson et al., 2000; Sahr et al., 2005). In 7-d-old pea (*Pisum sativum*) seedlings, it was shown that the root meristem contained 5-fold more folates than the mature root. The elevated level of folates in the root meristem was strongly correlated with high mRNA and protein expression of dihydropterin pyrophosphokinase-dihydropteroate synthase, an enzyme that catalyzes reactions specific to THF synthesis (Jabrin et al., 2003). In maize (*Zea mays*) roots, expression of the gene encoding the bifunctional dihydrofolate reductase and thymidylate synthase, which is involved in de novo generation of folate and thymidylate (Cossins, 2000; Fig. 1), was highest in the meristem but barely detectable in the elongation zone (Cox et al., 1999). These studies indicate that a steady pool of folate cofactors is essential to sustain actively dividing cells in the root tip. Indeed, pharmacological induction of folate deficiency in plants caused a reduction in cell division in Arabidopsis suspension cells and an inhibition of seedling growth (Loizeau et al., 2007, 2008; Raichaudhuri et al., 2009). In plants, both folate biosynthetic and folate-dependent enzymes are distributed among three cellular compartments: plastids, mitochondria, and the cytosol (Appling, 1991; Rébeillé et al., 2006; Loizeau et al., 2008; Fig. 1). However, the significance of folate compartmentation to plant development is not yet fully understood.

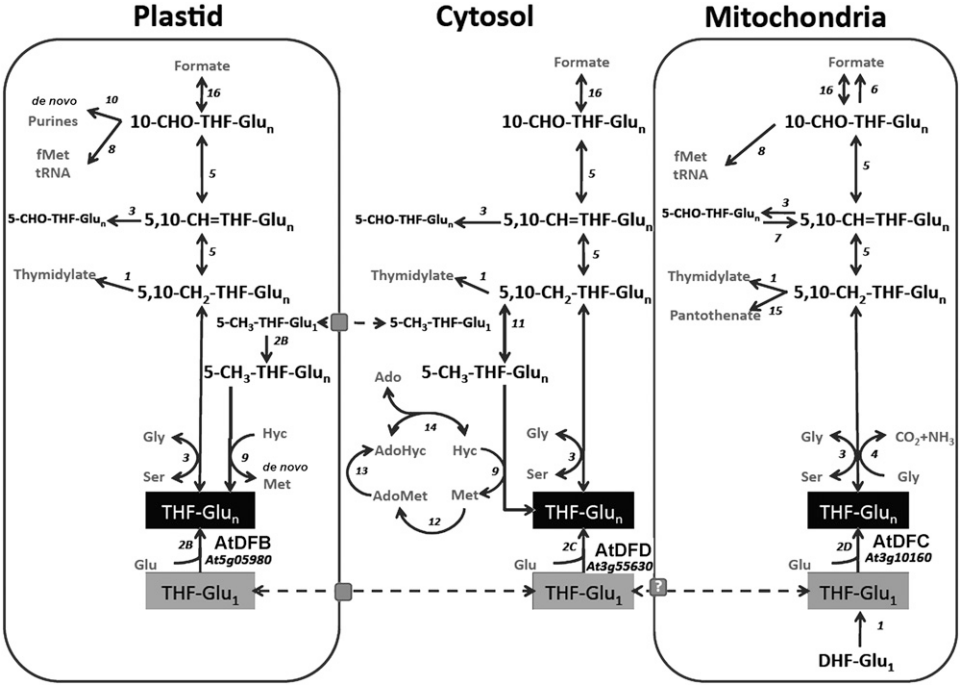

Figure 1. Schematic representation of THF production and C1 metabolism and their distribution in different compartments of the plant cell (adapted from Ravanel et al., 2001; Loizeau et al., 2008). Arrows and numbers represent enzymatic reactions. Dashed arrows and gray squares represent folate transport and transporters, respectively. 1, Dihydrofolate reductase/thymidylate synthase; 2, folylpolyglutamate synthetase (AtDFB, AtDFC, and AtDFD); 3, Ser hydroxymethyltransferase; 4, Gly decarboxylase; 5, 5,10-CH_2-THF dehydrogenase/5,10-CH-THF cyclohydrolase; 6, 10-formyl-THF deformylase; 7, 5-formyl-THF cycloligase; 8, methionyl-tRNA formyltransferase; 9, Met synthase; 10, glycinamide ribonucleotide transformylase and aminoimidazole carboxamide ribonucleotide transformylase; 11, 5,10-CH_2-THF reductase; 12, AdoMet synthetase; 13, Met *S*-methyltransferase; 14, *S*-adenosylhomocysteine hydrolase; 15, ketopantoate hydroxymethyltransferase; 16, 10-formyl-THF synthetase.

Although much progress has been made toward understanding the biochemistry of plant enzymes involved in folate biosynthesis and turnover (Ravanel et al., 2001; Hanson and Gregory, 2002), genetic evidence for the in planta functions of these enzymes is limited. In one study, the Arabidopsis *globular arrest1* mutant, which exhibited defective embryo development, was shown to be disrupted in the *AtDFA* gene (Ishikawa et al., 2003). In Arabidopsis, *AtDFA* is a single gene that encodes a functional mitochondrial matrix-localized dihydrofolate synthetase, which catalyzes the addition of the first glutamyl side chain to dihydropteroate to form dihydrofolate (Ravanel et al., 2001). Downstream of dihydrofolate synthetase is folylpolyglutamate synthetase (FPGS), an enzyme that catalyzes the sequential conjugation of additional Glu residues to the folate molecule to form folylpolyglutamates, the preferred substrates for several enzymes involved in C1 metabolism (Cossins and Chen, 1997; Ravanel et al., 2001; Fig. 1). Polyglutamylation is also essential for the retention of folates within a given cellular compartment, since organellar folate transporters are more specific to monoglutamylated folates (Bedhomme et al., 2005; Klaus et al., 2005; Raichaudhuri et al., 2009). In Arabidopsis, three genes, *AtDFB*, *AtDFC*, and *AtDFD*, have been reported to encode the plastidial, mitochondrial, and cytoplasmic FPGS isoforms, respectively (Ravanel et al., 2001; Fig. 1). In a recent reverse genetics study, different double mutant combinations to these Arabidopsis FPGS isoforms resulted in dramatic developmental phenotypes including embryo lethality, seedling lethality, late flowering, and dwarf plants with various reproductive defects (Mehrshahi et al., 2010). However, phenotypes were only reported in double *FPGS* mutants but not in single mutants, leading to the conclusion of redundancy in compartmentalized FPGS activity (Mehrshahi et al., 2010). Also in Arabidopsis, double mutants to genes encoding two 10-formyl-tetrahydrofolate (10-CHO-THF) deformylases (PurU) that metabolize 10-CHO-THF to formate and THF were smaller and paler compared with wild-type plants. In addition, double *PurU* mutants exhibited delayed embryo development and shriveled nonviable seeds (Collakova et al., 2008).

In this study, a forward genetic screen led to the identification of a recessive Arabidopsis mutant that exhibited stunted primary root and root hair growth. The mutant contained a T-DNA insertion in the *At5g05980* gene, which encodes the plastidial FPGS isoform designated as AtDFB for Arabidopsis DHS-FPGS isoform B (Ravanel et al., 2001) and recently renamed FPGS1 by Mehrshahi et al. (2010). The short primary root of *atdfb* was associated with a disorganized quiescent center (QC), reduced cell division and expansion, an extensively bundled actin cytoskeleton, and dissipation of the auxin gradient in the root cap. The *AtDFB* mutation led to changes in the glutamylation status of some folate classes that were coupled to a general depletion of amino acids and nucleotides, indicative of broad alterations in metabolism. The disorganized QC in *atdfb* was consistent with previous transcript profiling studies that showed strong *AtDFB* expression in the QC (Nawy et al., 2005) and therefore point to a role for metabolically active folates in maintaining QC function. No obvious defects in root development were observed in single mutants to *AtDFC* and *AtDFD*. Our data indicate that AtDFB is the predominant FPGS isoform that generates physiologically active folate cofactors required to sustain postembryonic root growth in developing Arabidopsis seedlings.

RESULTS

AtDFB Loss-of-Function Mutants Are Impaired in Primary Root Growth

We isolated a mutant originally designated as *drh2* (for *defective root hair2*) from a T-DNA activation-tagged population with root hairs that were wavy and short (Supplemental Fig. S1). It was also found that the mutant had significantly shorter primary roots than the wild type (Fig. 2A). The F2 generation segregated in a 3:1 (wild type:mutant) ratio after crossing the mutant to the wild type, consistent with a single recessive mutation. Closer examination of the primary roots of 7-d-old seedlings showed a shorter growth zone in *drh2*, as evident from the emergence of root hairs very close to the root tip (Fig. 2A). In 11-d-old seedlings, roots of the wild type were more than 8-fold longer than *drh2* and formed about two adventitious roots (Fig. 2B). At 3 to 8 d, primary root growth rate of *drh2* was only 1.67 ± 0.09 mm d^{-1} but increased to 4.40 ± 0.31 mm d^{-1} by 15 to 17 d (Fig. 2C). In wild-type seedlings, primary root growth rate was 8.35 ± 0.46 mm d^{-1} in 3- to 8-d-old seedlings and decreased to 7.02 ± 0.37 mm d^{-1} in 15- to 17-d-old seedlings (values are means of 20 roots $\pm$ SE).

Thermal asymmetric interlaced PCR of the *drh2* mutant identified a T-DNA insert in the fifth intron of the *At5g05980* gene, which encodes AtDFB (Ravanel et al., 2001). SAIL_556_G08 and SALK_015472 were identified as additional lines with T-DNA insertions in the sixth intron and eighth exon of *At5g05980*, respectively, and both lines exhibited root phenotypes similar to those of *drh2*, indicating that the defective primary root and root hair growth exhibited by the *drh2* seedlings was due to mutations in the *AtDFB* gene. *Drh2*, SAIL_556_G08, and SALK_015472 were therefore designated as *atdfb-1*, *atdfb-2*, and *atdfb-3*, respectively (Fig. 3, A and B). Reverse transcription (RT)-PCR analysis showed that *atdfb-1*, *atdfb-2*, and *atdfb-3* had no detectable transcript using primers flanking the T-DNA insertion (Fig. 3C). Despite the short primary root of *atdfb*, no obvious defects in the development of the aboveground organs were observed (Supplemental Fig. S2).

Real-time quantitative RT-PCR analysis revealed that *AtDFB* was expressed in both shoots and roots,

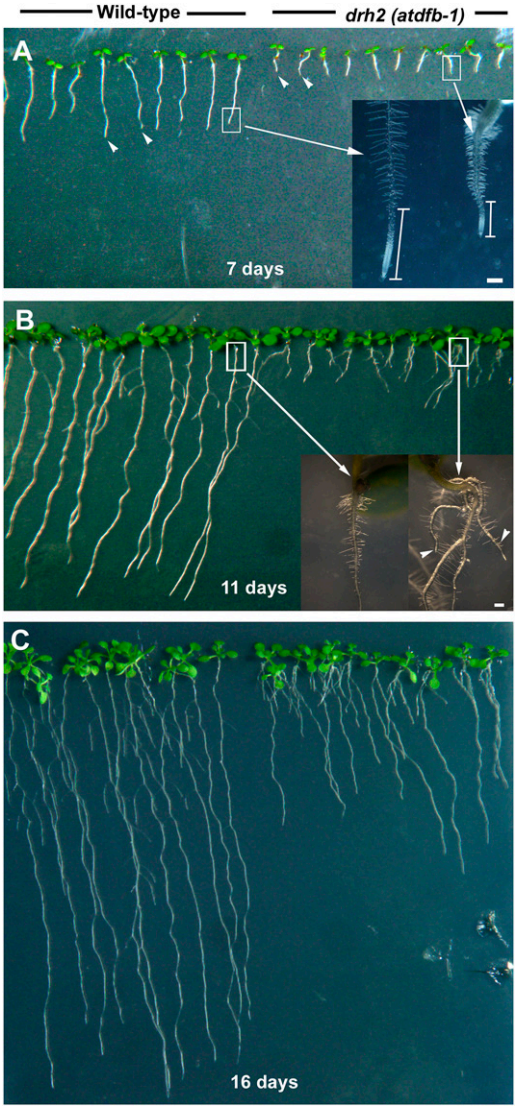

Figure 2. Primary root defects of *drh2*. A, Seven-day-old wild-type and mutant seedlings. The primary root length of the mutant is about 4-fold less than that of the wild type (arrowheads). The shorter primary root of *drh2* was due to a reduced growth zone, as indicated by the emergence of root hairs closer to the root tip compared with the wild type (white vertical bars in the inset). B, In 11-d-old seedlings, differences in root architecture between the wild type and mutant become more apparent. In addition to the short primary root, *drh2* seedlings had about two adventitious roots (arrowheads in the inset) while wild-type seedlings had none. C, At 16 d, *drh2* primary roots started to elongate faster compared with the earlier stages of seedling development but were still significantly shorter than in the wild type. Bars = 200 μm for insets in A and B.

but expression in roots was higher compared with shoots (Fig. 4A). Whole mount in situ hybridization using gene-specific probes confirmed stronger expression of *AtDFB* in the root apex compared with shoots (Fig. 4, B–D). Furthermore, previous transcript profiling of GFP-marked root cell types in Arabidopsis revealed that *AtDFB* was strongly expressed in the QC (Nawy et al., 2005). In agreement with these results, distinct *AtDFB* expression was observed in the QC region of the root tip (Fig. 4C).

AtDFC and *AtDFD* encode two other FPGS isoforms that have been reported to localize to the mitochondria and cytoplasm, respectively (Ravanel et al., 2001; Fig. 1). No obvious defects in root development were observed in single mutants to these other FPGS isoforms (Supplemental Fig. S3). The higher root expression of *AtDFB* compared with *AtDFC* and *AtDFD*, as shown by publicly available Arabidopsis microarray expression data sets from Genevestigator (Supplemental Fig. S4; Zimmermann et al., 2004), supports our findings that AtDFB plays a more important role in root development than the other two FPGS isoforms.

The Short-Root Phenotype of *atdfb* Is the Result of Reduced Cell Division and Cell Expansion

We next determined whether the short primary root of *atdfb* was the result of reduced cell division and/or expansion. Differential interference contrast images of

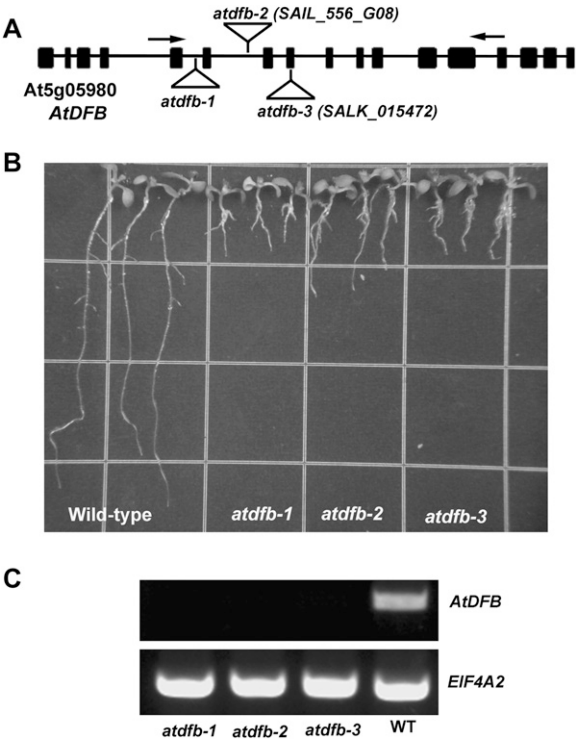

Figure 3. A, Schematic diagram of the genome organization of *AtDFB*. *drh2* had a T-DNA insertion in the fifth intron of the *At5g05980* gene, which encodes AtDFB. Boxes indicate exons and lines indicate introns. The T-DNA insertion sites for each of the mutant alleles are indicated. B, Twelve-day-old seedlings of the wild type, *atdfb-1*, *atdfb-2*, and *atdfb-3*. Note the severely reduced primary root length of all mutant alleles. C, Semiquatitative RT-PCR of *AtDFB* in the wild type (WT), *atdfb-1*, *atdfb-2*, and *atdfb-3*. Total RNA was prepared from 7-d-old seedlings, and arrows in A indicate the positions of the primers used for RT-PCR. *EIF4A-2* primers were used as a control.

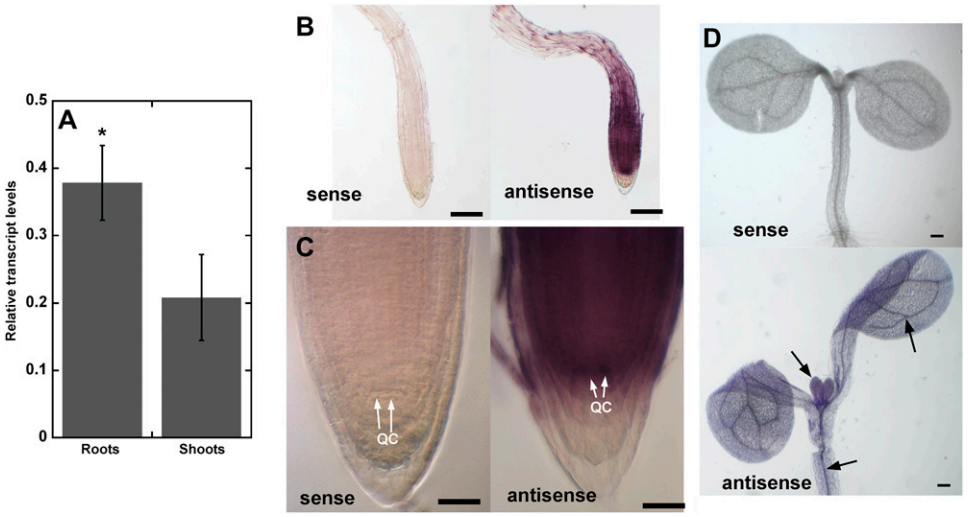

Figure 4. Expression of *AtDFB* in 7-d-old wild-type Arabidopsis seedlings revealed by quantitative RT-PCR and whole mount RNA in situ hybridization. A, Quantitative RT-PCR shows that *AtDFB* is more strongly expressed in roots compared with shoots. Values are means ± SE of three independent biological replicates (each replicate had 40 seedlings for RNA extraction). The asterisk indicates a statistically significant difference according to Student's *t* test ($P < 0.05$). B to D, *AtDFB* transcript is visible as a purple signal in bright-field images of the root apex hybridized with antisense but not with sense probes. Note the strong purple staining in the QC. A purple precipitate was also observed in vascular tissues of the cotyledons and hypocotyls, and the first true leaves of 7-d-old seedlings hybridized with antisense probes (arrows in D). Bars = 100 μm (B and D) and 25 μm (C).

the epidermal cells from the root hair region were acquired and their lengths measured. From the differential interference contrast images, it was obvious that epidermal cells of wild-type roots were two times longer than epidermal cells of *atdfb-1* roots (Fig. 5, A and B). The average epidermal cell length of wild-type seedlings was 154.4 ± 34.8 μm compared with 74.1 ± 2.4 μm in *atdfb-1*(Fig. 5C; values are means ± SE of 40–50 cells from 10–12 seedlings).

Because the actin cytoskeleton is an important regulator of cell expansion (Blancaflor et al., 2006), we asked if the short primary roots of *atdfb-1* was impaired in F-actin organization. In wild-type seedlings, cells in the root elongation zone consisted of randomly organized fine F-actin arrays, a typical feature of actin organization in wild-type roots (Fig. 5D; Wang et al., 2008). On the other hand, F-actin in the shorter epidermal cells of *atdfb-1* roots was extensively bundled (Fig. 5E). Bundling and fluorescent aggregates were also observed in the interphase cells within the root meristem of *atdfb-1* but not in the wild type (Fig. 5, F and G). In addition, cells that were undergoing cytokinesis in wild-type roots could be easily identified by the presence of GFP-labeled F-actin in the phragmoplast (Fig. 5F). F-actin-labeled phragmoplasts were rarely observed in the meristem of *atdfb-1* roots (Fig. 5G).

The scarcity of F-actin-labeled phragmoplasts (Fig. 5G) in *atdfb-1* roots strongly suggested that cell division was impaired. Consistent with the F-actin labeling result, the average number of mitotic cells in 5-d-old 4′,6-diamidino-2-phenylindole (DAPI)-stained roots of *atdfb-1* seedlings was significantly less than in the wild type (Fig. 5H). Taken together, these cellular assays indicated that the reduced primary root growth of *atdfb-1* can be attributed to defects in both cell division and cell expansion.

Postembryonic QC Organization and Auxin Gradients Are Altered in Roots of *atdfb*

Because the QC plays a crucial role in root meristem maintenance by serving as a source for replenishing expiring cell initials (van den Berg et al., 1997), it is possible that altered QC function is one cause of the impaired cell division in *atdfb-1*, given the strong expression of *AtDFB* in the QC (Nawy et al., 2005; Fig. 4C). Indeed, it was found that unlike wild-type roots, which clearly showed the two- to four-cell QC typically observed in median confocal sections of propidium iodide-stained roots (Nawy et al., 2005; Fig. 6A), cells in the root apex of 5-d-old *atdfb-1* seedlings that corresponded to the QC region of wild-type roots were disorganized (Fig. 6B). However, no gross differences in the organization of cells in the QC region of mature embryos were observed between wild-type and *atdfb* roots (Fig. 6, C and D), which appeared to persist for up to 3 to 4 d post germination (Fig. 6, E and F). Clear differences in QC organization between the wild type and *atdfb-1* only became obvious in seedlings older than 4 to 5 d.

Another important regulator of root development is the plant hormone auxin. In Arabidopsis roots, local auxin concentration gradients have been shown to direct patterns of cell division, expansion, and differentiation in the root apex (Overvoorde et al., 2010). Therefore, we investigated whether the root defects of *atdfb* were associated with altered local auxin gradi-

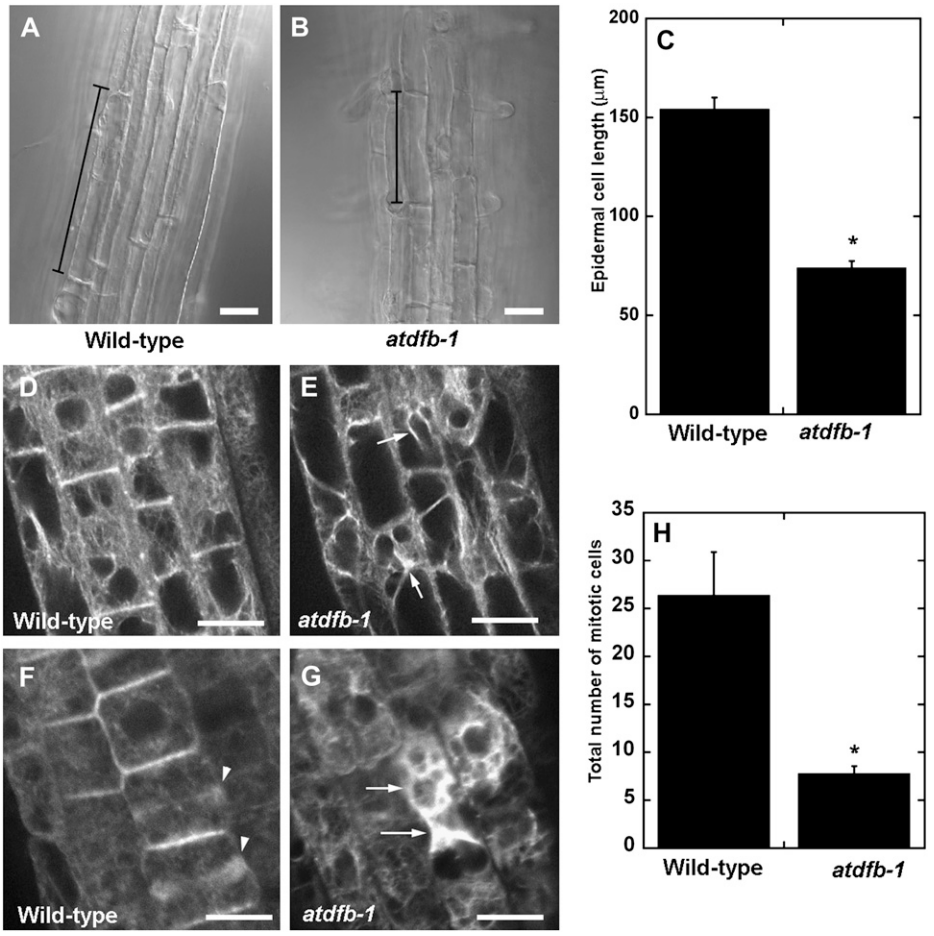

Figure 5. Cell expansion, cell division, and F-actin organization are altered in roots of *atdfb-1*. A and B, Epidermal cells of wild-type roots in the maturation zone (A) are longer than those of *atdfb* (B). Black vertical bars mark the end walls of a representative epidermal cell. C, Quantification of epidermal cell length in the maturation zone shows that wild-type cells are more than 2-fold longer than mutant cells. Values are means ± SE of 40 epidermal cells from 10 roots. D to G, The actin cytoskeleton in the elongation zone (D and E) and the meristem (F and G) of the wild type and *atdfb-1*. Note the bundling of F-actin in mutant root cells (arrows in E and G). The meristem region of wild-type roots is enriched in F-actin-labeled phragmoplasts (arrowheads in F) but absent in *atdfb-1* (G). H, The number of mitotic cells is significantly reduced in roots of *atdfb* compared with the wild type. Values are means ± SE of five root tips. Asterisks in C and H indicate statistically significant differences according to Student's *t* test ($P < 0.01$). Bars = 20 μm (A and B) and 10 μm (D–G).

ents. For these studies, we used the synthetic auxin-responsive reporter *DR5*:*GFPm*, which indirectly reports patterns of local auxin accumulation in Arabidopsis roots (Ottenschläger et al., 2003). Roots from 8-d-old wild-type seedlings showed *DR5*:*GFPm* expression in both the QC and central cells of the columella (Fig. 7A). In contrast, the expression of *DR5*:*GFPm* in roots of *atdfb-1* was confined to only a few cells in the columella (Fig. 7B). The number of cells expressing *DR5*:*GFPm* in median confocal sections of the root cap of 8-d-old *atdfb-1* seedlings was about 3-fold less than that of the wild type (Fig. 7C).

Another function of the QC is the generation of cell-autonomous signals that suppress differentiation and therefore maintain the adjacent stem cells (van den Berg et al., 1997). In Arabidopsis roots where the QC was removed by laser ablation or in mutants that were unable to specify a QC, the ability to maintain the surrounding columella initials was compromised (van den Berg et al., 1997; Sabatini et al., 2003). In the root cap, differentiation into columella cells is marked by the formation of starch-filled amyloplasts that can be readily imaged by Lugol staining. In this and other studies, it was shown that columella initials of wild-type roots proximal to the QC typically lacked amyloplasts (Fig. 7D; Sabatini et al., 2003). However, similar to roots with a defective QC (Sabatini et al., 2003), cells immediately below the disorganized QC region of *atdfb* acquired the amyloplast differentiation markers that are typically only expressed in mature columella cells (Fig. 7E). Furthermore, real-time quantitative RT-PCR of the *AGAMOUS-LIKE42* (*AGL42*) gene, which is a marker for the QC (Nawy et al., 2005), was significantly reduced in root tips of *atdfb-1* (Fig. 7F).

5-CHO-THF Rescues the Root Growth Defects of *atdfb*

We next tested whether the exogenous application of a stable form of THF such as 5-CHO-THF could rescue the *atdfb* root defects. 5-CHO-THF has been used to rescue the inability of cultured *globular arrest1* embryos, which are defective in the gene encoding *AtDFA*, to form calli (Ishikawa et al., 2003) and partially rescue the developmental defects of Arabidopsis FPGS double mutants (Mehrshahi et al., 2010). When all three mutant alleles of *AtDFB* were planted on medium supplemented with 500 μM 5-CHO-THF, their primary roots were restored to wild-type lengths (Fig. 8, A and B). The restoration of root growth of *atdfb-1* to the wild type upon exposure to 5-CHO-THF was also accompanied by the reformation of wild-type QC organization (Fig. 8C) and a corresponding increase

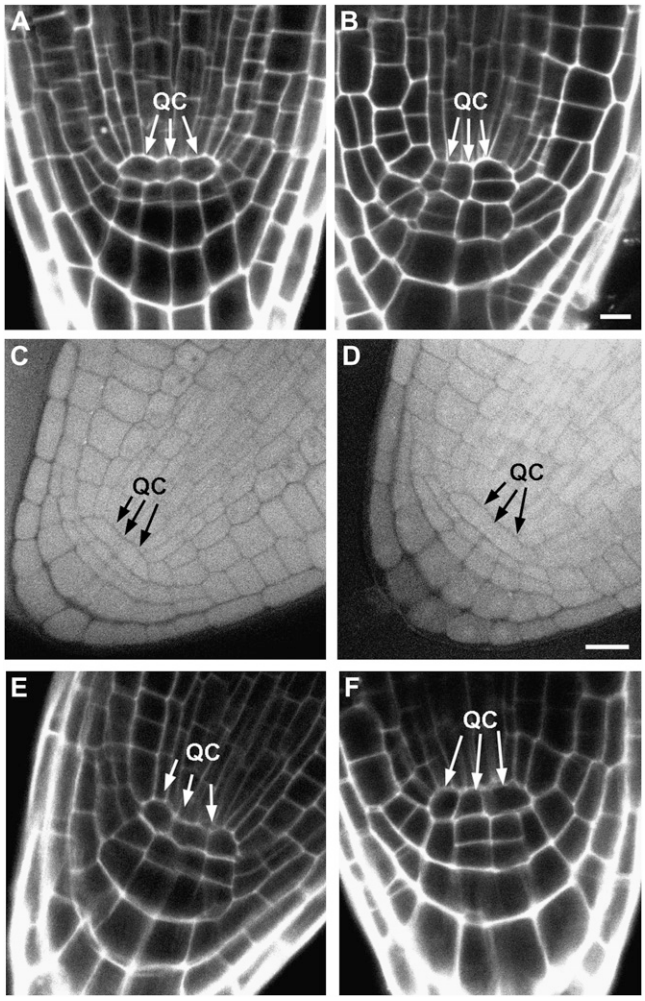

Figure 6. The QC is disorganized in postembryonic roots of *atdfb*. A, Median confocal image of a 5-d-old propidium iodide-stained wild-type root clearly shows a well-organized QC (arrows). B, In *atdfb-1* roots, cells in the region corresponding to the QC have a disorganized pattern (arrows). C to F, In mature embryos (C and D) and roots from 2-d-old seedlings (E and F), QC organization in the wild type (C and E) appears similar to *atdfb-1* (D and F). Bars = 10 μm.

in the number of mitotic cells (Supplemental Fig. S5A). In addition, the average root hair length of *atdfb* increased significantly compared with untreated seedlings and was almost restored to wild-type lengths (Supplemental Fig. S5, B and C).

To better understand why 5-CHO-THF, which is not a C1 donor, was able to chemically complement the root phenotype of *atdfb*, we analyzed total folates in roots of the rescued seedlings. It was found that a massive (greater than 2,300-fold) increase in total folate occurred in 5-CHO-THF-supplemented roots compared with nonsupplemented roots in both wild-type and *atdfb-1* seedlings. Individual folate classes accumulated in 5-CHO-THF-treated seedling roots showed similar contributions to the folate pool than those observed in solvent controls with 5-CH_3-THF as the most predominant folate that accumulated (Supplemental Fig. S5D).

The Folate Glutamylation Profile Is Altered in *atdfb* Seedlings

To determine the impact of the *AtDFB* mutation on folate metabolism, folate analyses were performed on shoots and roots of 15-d-old seedlings. Total folate content did not significantly change between the wild type and *atdfb-1* in both shoots and roots. However, we did find differences in the accumulation patterns of some folate classes and general changes in the contribution of each folate class to the total folate pool (Supplemental Table S1).

Because AtDFB catalyzes the extension of the Glu tail of the folate molecule (Ravanel et al., 2001; Fig. 1), differences in the glutamylation state of folates between wild-type and *atdfb-1* seedlings might be predicted rather than differences in total folate content. Indeed, a considerable increase in total monoglutamylated folates in *atdfb* roots when compared with wild-type roots was found (Fig. 9B). This difference was not observed in shoots (Fig. 9A), and polyglutamylated total folate content was not altered in either tissue (Fig. 9, C and D). However, when we looked at the individual folate classes, the glutamylation state of some folate classes was significantly different between wild-type and *atdfb-1* seedlings (Fig. 9). The most significant difference was an increase in monoglutamylated 5-CH_3-THF, from 9% of the total 5-CH_3-THF pool in wild-type roots to 53% in *atdfb-1* roots (Student's *t* test, $\alpha = 0.05$, $P \leq 0.0006$; Fig. 9B). The root glutamylation profile of 5,10-CH-THF (5,10-CH=THF), which is the sum of the conversion of 10-CHO-THF at acidic pH and the existing 5,10-CH=THF pool (Quinlivan et al., 2006), was also impacted by the *AtDFB* mutation. Roots of *atdfb-1* had 77% of the 5,10-CH=THF pool in the monoglutamylated form as opposed to the wild type, which had only 44% of the 5,10-CH=THF pool in the monoglutamylated form (Fig. 9B).

Although the level of monoglutamylated 5-CH_3-THF in both shoots and roots of *atdfb-1* was generally higher than in the wild type (Fig. 9, A and B), the polyglutamylation level of this folate class was not significantly different between the wild type and *atdfb-1* (Fig. 9, C and D). However, polyglutamylation levels of 5,10-CH=THF were significantly lower in both shoots and roots of *atdfb-1* compared with the wild type (Fig. 9, C and D). A 7-fold increase in levels of 5-CHO-THF was also detected in *atdfb-1* roots compared with the wild type, with more than 90% of this increase in the polyglutamylated form (Fig. 9D).

Amino Acids and Nucleotides Are Depleted in Whole Seedlings of *atdfb*

Nontargeted metabolic profiling of 7-d-old whole Arabidopsis seedlings was performed using gas chromatography-mass spectrometry (GC-MS) to determine how the *AtDFB* mutation impacted overall metabolism. A total of 776 polar and 415 nonpolar compounds were detected in *atdfb-1* and wild-type seedlings, respec-

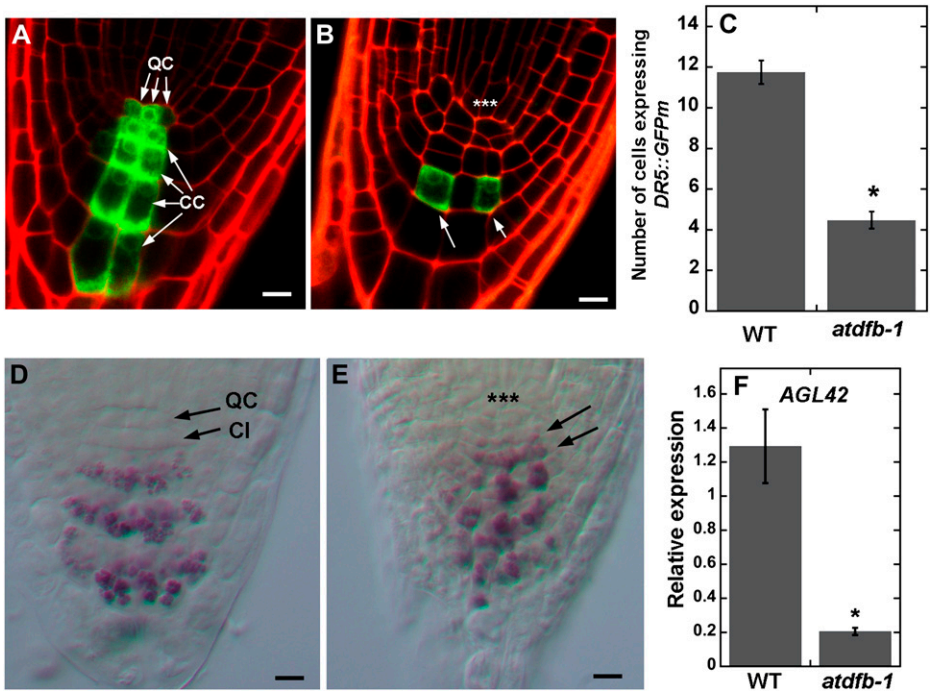

Figure 7. *DR5:GFPm* expression and QC identity are altered in *atdfb* roots. A, Root cap of an 8-d-old wild-type seedling shows *DR5:GFPm* expression in the QC and central columella cells (CC). B, In 8-d-old *atdfb-1* seedlings, *DR5:GFPm* expression is confined to a few columella cells (arrows). Note the disorganized QC region in *atdfb-1* (asterisks). C, More cells in the root cap express *DR5:GFPm* in wild-type seedlings (WT) compared with *atdfb-1*.Values are means from 15 roots ± SE. The asterisk indicates a statistically significant difference (Student's *t* test, $P < 0.01$). D, Purple-stained amyloplasts are absent in columella initials (CI) of wild-type seedlings. E, In roots of *atdfb-1*, amyloplasts (arrows) prematurely form close to the disorganized cells in the QC region (asterisks). F, Quantitative RT-PCR shows higher expression of the QC-expressed gene *AGL42* in 8-d-old roots of the wild type compared to *atdfb-1*. Values are means ± SE of five biological replicates. The asterisk indicates a statistically significant difference according to Student's *t* test ($P < 0.05$). Bars = 10 μm.

tively, of which 193 polar compounds and 92 nonpolar compounds could be assigned a chemical structure based on electron ionization-MS spectral matching to authentic compounds (Supplemental Tables S2 and S3).

Hierarchical clustering analysis using a green-black-red diagram was used to illustrate the distribution of normalized signal intensities of cellular metabolites in the wild type and *atdfb-1*. This analysis showed that nucleotides and amino acids were generally depleted in *atdfb-1* (Fig. 10A). Amino acids that showed a statistically significant reduction in *atdfb-1* compared with the wild type included Cys, Arg, Gln, Asn, Met, Phe, Lys, and Tyr (Fig. 10B). Folates serve as cofactors for Met biosynthesis and Ser-Gly interconversion (Hanson and Roje, 2001; Fig. 1). However, we did not find any significant differences in Ser and Gly levels between wild-type and *atdfb-1* seedlings (Fig. 10C). For nucleotides, statistically significant reductions in the levels of guanosine, adenine, uridine, UMP, and 5-methyl pyrimidine were noted (Fig. 10, D and E).

Exogenous Met and Guanosine Partially Alleviate the Root Growth Defects of *atdfb*

Metabolic profiling showed that endogenous Met levels in *atdfb-1* seedlings were lower relative to the wild type (Fig. 10B). In yeast, *met7*, a mutant disrupted in a gene encoding a cytosolic FPGS, requires a source of external Met for growth (Cherest et al., 2000). Expressing the *AtDFB* gene in *met7* abolished its dependence on external Met (Ravanel et al., 2001). Therefore, we tested whether the application of exogenous Met could rescue the root defects of *atdfb*. It was found that Met concentrations of 10 to 25 μM induced a more than 2-fold increase in root growth of *atdfb-1* compared with the nontreated *atdfb-1* controls (Supplemental Fig. S6A). Although root growth of *atdfb-1* seedlings was clearly promoted upon exposure to Met, their roots remained significantly shorter than wild-type roots grown with or without external Met (Supplemental Fig. S6B).

We also tested whether supplying seedlings with external adenine or guanosine had any effect on roots of *atdfb-1*, given the reduction in the levels of these metabolites in the mutant compared with the wild type (Fig. 10E). Exogenous guanosine at 10 nM induced a slight but statistically significant increase in root length of *atdfb-1*. However, 10 μM external guanosine did not impact root growth of *atdfb-1* (Supplemental Fig. S6C). Unlike Met and guanosine, adenine did not promote root growth of the mutant (Supplemental Fig. S6C). A combination of adenine, guanosine, and Met induced a

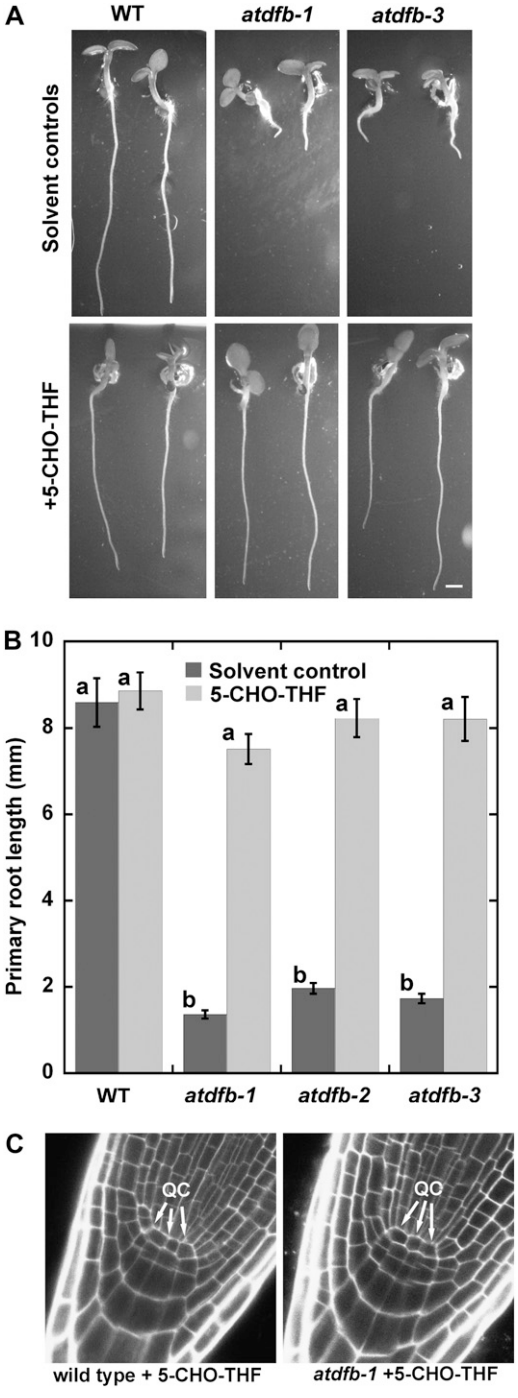

Figure 8. Exogenous 5-CHO-THF rescues the short primary root phenotype of *atdfb*. A and B, Seven-day-old seedlings of the wild type (WT) and *atdfb* germinated in solvent control and 500 μM 5-CHO-THF. Note that the primary root length of *atdfb* is restored to the wild type. Data are means from 18 to 25 roots ± SE. Means with different letters are statistically significant (Tukey's test, $P < 0.05$). C, QC organization in *atdfb* is also restored to wild-type patterns when grown on 500 μM 5-CHO-THF.

statistically significant increase in *atdfb-1* root length compared with controls, but the induction of growth was similar to either Met or guanosine alone (Supplemental Fig. S6C).

DISCUSSION

Three genes in Arabidopsis encode FPGS isoforms that were previously shown to localize to different cellular compartments (Ravanel et al., 2001). In a recent reverse genetics study, various double mutant combinations of these Arabidopsis FPGS isoforms resulted in dramatic developmental phenotypes, providing compelling evidence for the importance of polyglutamylated folates in plant development (Mehrshahi et al., 2010). However, because single FPGS mutants did not appear to have any obvious defects in the aboveground organs of mature plants that were grown directly from soil, it was concluded that redundancy in compartmentalized FPGS activity is likely operating during plant development (Mehrshahi et al., 2010). In this study, we show that disruption of a gene encoding a single FPGS isoform (*AtDFB*) resulted in a dramatic reduction in primary root elongation. Because single *AtDFC* and *AtDFD* mutants had no obvious primary root defects (Supplemental Fig. S3), our data indicate that *AtDFB* is the predominant FPGS isoform that generates the bulk of polyglutamylated folate cofactors for C1 metabolism required to sustain normal meristematic activity and cell expansion in actively growing root tips.

The importance of *AtDFB* for root development is supported by its strong expression in the root QC (Nawy et al., 2005; Fig. 4). Loss of *AtDFB* function could theoretically compromise regenerative cell divisions of the QC and explain the various root cell defects of *atdfb*. Indeed, it was found that cells in the QC region of *atdfb* were disorganized, and this was coupled to altered gradients of the auxin-sensitive *DR5*:*GFPm*, reduced expression of the QC-expressed gene, *AGL42* (Nawy et al., 2005), and premature formation of amyloplast differentiation markers. In this regard, it is noteworthy that genetic disruption of *DR5* expression and mutations that resulted in loss of QC identity led to short primary roots and cell patterning abnormalities reminiscent of *atdfb* defects (Sabatini et al., 1999, 2003). Furthermore, the adventitious root phenotype of *atdfb* mirrored that of *short root*, which is consistent with the loss of root apical meristem activity (Lucas et al., 2011).

The lack of any obvious embryonic and shoot defects in *atdfb* supports recent reverse genetic studies suggesting that *AtDFC* or *AtDFD* is able to compensate for the absence of *AtDFB* during embryo and aboveground vegetative development (Mehrshahi et al., 2010). However, a novel finding from our studies is that these other FPGS isoforms do not always function redundantly, at least within a specific window of postembryonic root development. During this developmental window, the QC-expressed AtDFB isoform plays a major role in maintaining QC identity to support normal meristematic function during postembryonic root growth. We cannot rule out the possibility that QC identity in *atdfb* is already impacted before defects in cell organization within the QC region become apparent. Future studies will examine the spatial and temporal expression of

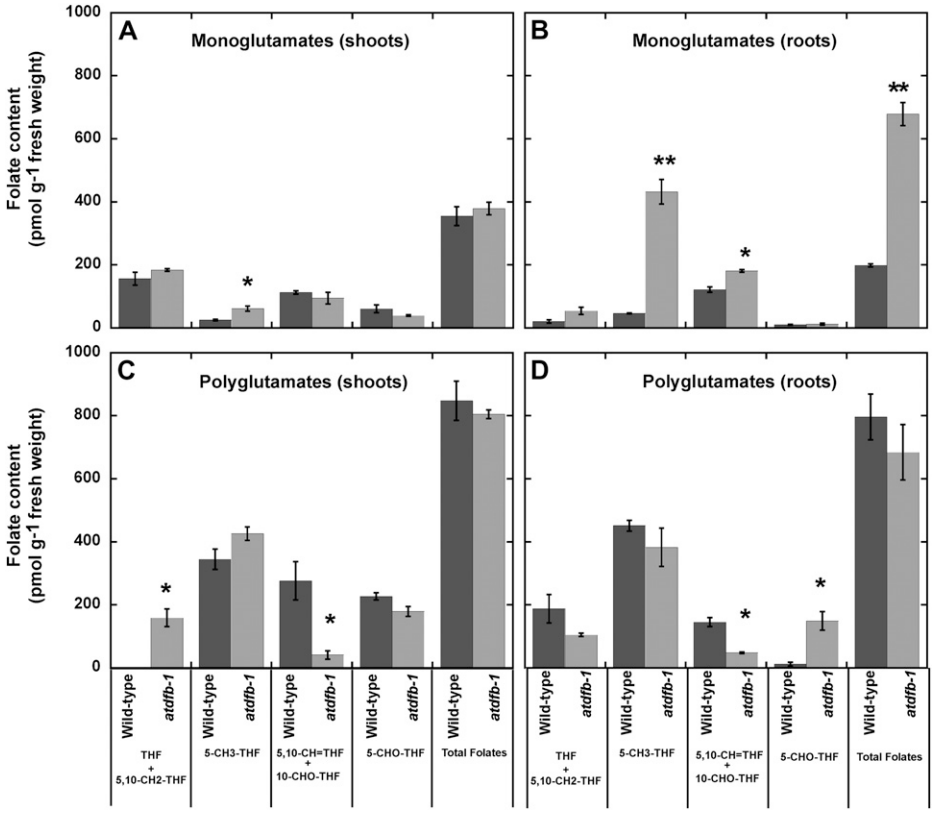

Figure 9. Folate glutamylation profile in shoots and roots of 15-d-old Arabidopsis seedlings. Each folate class and total folates are presented as monoglutamates (A and B) or polyglutamates (C and D). Monoglutamyl contribution to each folate class was calculated by subtracting deglutamylated values from monoglutamyl quantification in polygutamylation profile analysis. Data are means ± SE of three independent preparations. Asterisks indicate statistically significant differences (Student's *t* test, * $P < 0.05$, ** $P < 0.001$).

several QC identity markers (Sabatini et al., 2003; Nawy et al., 2005) in *atdfb* mutants at different stages of embryonic and postembryonic root development to better understand the dynamics of QC function in relation to folate metabolism. It also is not clear whether AtDFB acts exclusively within the QC, since expression data suggest that it could be required for normal function of other cell types within the root meristem (Fig. 4; Supplemental Fig. S4).

Because folate monoglutamates that accumulated in *atdfb* cannot be efficiently utilized by folate-requiring enzymes (Appling, 1991; Sahr et al., 2005), biochemical processes in the root apex that require C1 metabolites may not function optimally, leading to the root defects of *atdfb*. On the other hand, differences in polyglutamylated folates between the wild type and *atdfb*, which were absent in whole root folate-profiling experiments, could be more pronounced in plastids, where *AtDFB* was shown to localize (Ravanel et al., 2001). Indeed, Mehrshahi et al. (2010) found that chloroplasts in mature leaves of *atdfb* had lower polyglutamylated folates than the wild type, but even within this compartment, polyglutamylated folate content was not totally abolished in the mutants. This led to the proposal that different FPGS isoforms might be targeted to more than one compartment or that plants have a mechanism for transporting folate polyglutamates (Mehrshahi et al., 2010). Given that the root developmental defects of *atdfb* can be traced in part to a defined group of cells that constitute the QC, whole root folate quantification could dilute differences in the folate polyglutamylation profiles between the wild type and *atdfb*. Thus, it will be necessary to develop sensitive methods to quantify folates from plastids of specific root cell types to better understand how metabolic changes within a defined group of cells translate into whole organ development.

Closer examination of individual folate classes revealed higher monoglutamylated and lower polyglutamylated 5,10-CH=THF in *atdfb-1* roots compared with the wild type (Fig. 9, B and D). In this regard, it is worth noting that the main form of folate found in chloroplasts is polyglutamylated 5,10-CH=THF, which comprises both 5,10-CH=THF and 10-CHO-THF (Klaus et al., 2005; Orsomando et al., 2005, Mehrshahi et al., 2010). In Arabidopsis, de novo purine biosynthesis occurs in plastids and requires 10-CHO-THF in two transformylation steps (Zrenner et al., 2006). A reduction of polyglutamylated 10-CHO-THF could prevent its retention within plastids and thus hinder its efficiency to be used as a cofactor in reactions leading to the biosynthesis of purines (Zrenner et al., 2006; Fig. 1). Indeed, it was found that endogenous levels of adenine and guanosine were reduced in *atdfb* seedlings (Fig. 10).

We did not find significant changes in THF + 5,10-CH_2-THF polyglutamylation levels in *atdfb* roots compared with the wild type (Fig. 9D). However, mutant shoots showed an increase in polyglutamylated forms of these folate classes (Fig. 9C), suggesting that THF

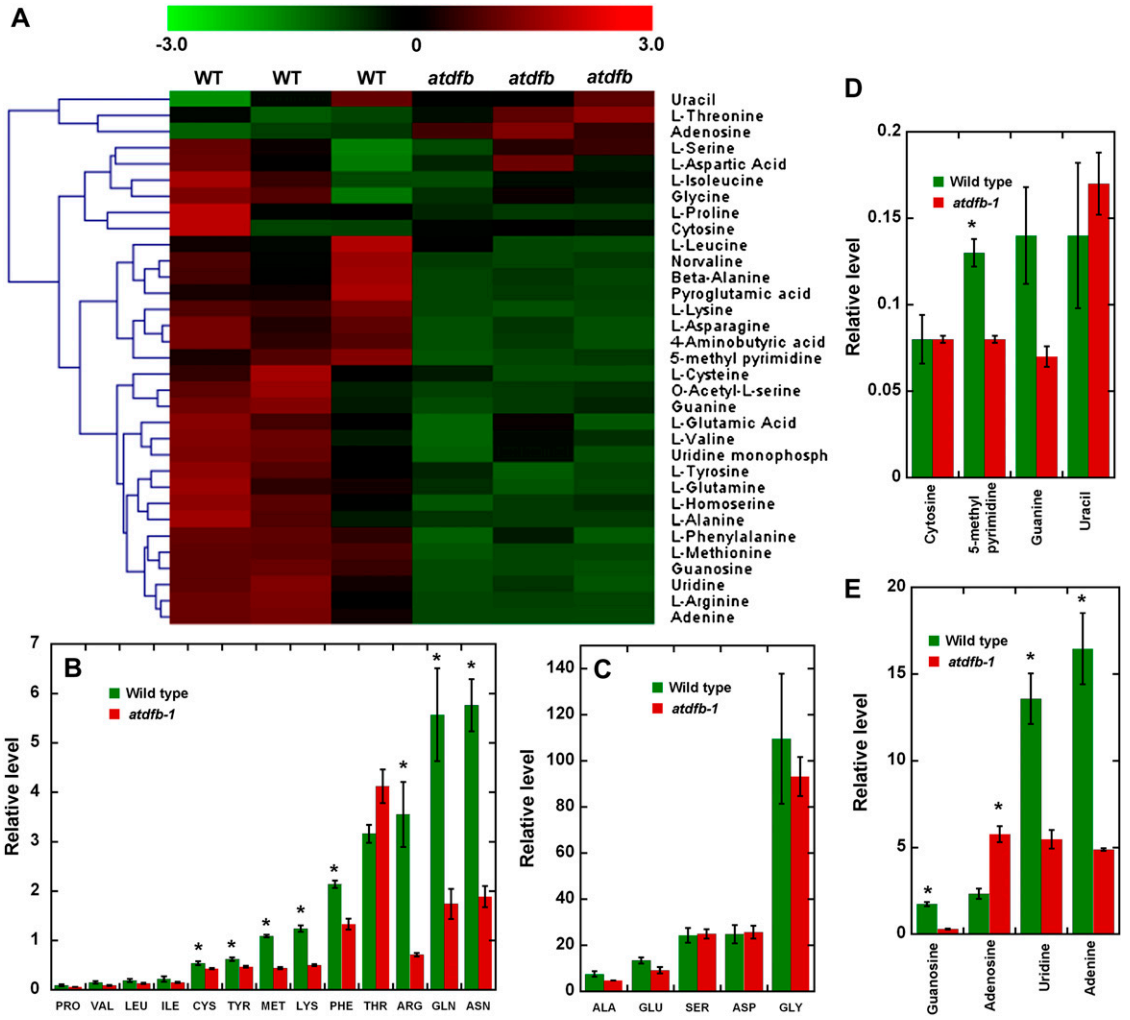

Figure 10. Metabolite profiling in whole seedlings of the wild type and *atdfb-1*. A, Heat map visualization of nucleotides and amino acids in 7-d-old seedlings of *atdfb-1* and the wild type (WT). Each biological replicate is visualized in a single column (average of $n = 3$). Red indicates high abundance, whereas metabolites in low abundance are in green. B to E, Alterations in mean amino acid levels (B and C) and mean nucleic acids (D and E) of *atdfb-1* compared with the wild type (Student's *t* test, * $P < 0.05$). For visual clarity, amino acids and nucleotides are presented in two groups based on their relative values.

and 5,10-CH_2-THF did not accumulate predominantly in plastids as shown previously (Orsomando et al., 2005; Mehrshahi et al., 2010). These two folate classes are involved in Ser-Gly interconversion by the action of Ser hydroxymethyltransferase (Besson et al., 1995), which is present in different cell compartments, including plastids (Hanson and Roje, 2001; Zhang et al., 2010; Fig. 1). These observations are consistent with the maintenance of a Ser-Gly pool that we found in mutant whole seedlings (Fig. 10C), which could be due to other Ser hydroxymethyltransferase isoforms acting outside plastids.

We also found a 7-fold increase of 5-CHO-THF in *atdfb* roots, with more than 90% of this increase in the polyglutamylated form (Fig. 9D). Polyglutamylated 5-CHO-THF was found to be a major folate in leaf mitochondria (Goyer et al., 2005; Orsomando et al., 2005). Thus, it is possible that reduction of polyglutamylation in plastids induced a redirection of folate flux, which then caused an accumulation of this folate class in roots. In fact, the contribution of each folate class to the total folate pool changed in the mutant in both shoots and roots (Supplemental Table S1), suggesting that the absence of AtDFB generates changes in the distribution and interconversion of folate pools within the cell. In this respect, previous work in Chinese hamster ovary cells showed that changes in mitochondrial and cytosolic FPGS activities caused clear folate redistribution between cell compartments (Lin et al., 1993; Qi et al., 1999). 5-CHO-THF does not participate in C1 reactions, and its role in planta is not very well understood. In fact, this folate species has been shown to inhibit the activity of many folate-utilizing enzymes (Stover and Schirch, 1993; Roje et al., 2002). Therefore, it was interesting to find that exogenous 5-CHO-THF rescued the root defects of *atdfb*

(Fig. 8). When we analyzed these chemically complemented mutant seedlings, we found that they accumulated more than 1,900 nmol g^{-1} folates, which is far above all natural folate levels reported (Supplemental Fig. S5D). This indicates that the exogenously supplied 5-CHO-THF was effectively taken up and converted into metabolic active folates by 5-formyl-THF cycloligase (Goyer et al., 2005; Fig. 1). This conversion occurred quite efficiently, because 5-CHO-THF represented less than 18% of the accumulated folates, with 5-CH_3-THF being the most predominant folate class in the total folate pool (Supplemental Fig. S5D). Thus, the recovery of root growth in *atdfb* treated with 5-CHO-THF was most likely due to the excess of folates in the monoglutamylated form, which might be able to complement the mutation by accomplishing the same functions as a small amount of polyglutamylated folates. Additionally, these results demonstrate the high capacity of the seedling to metabolize and accumulate large amounts of folates without apparent negative effects.

The depleted levels of amino acids and nucleotides are likely contributors to the defective root growth of *atdfb*. However, because metabolic profiling was done on whole seedlings, only part of the reported metabolic changes in the mutant can be attributed to folate polyglutamylation defects in roots. Met in particular is an essential amino acid required for protein synthesis and the formation of *S*-adenosylmethionine (AdoMet), the universal methyl donor in the methylation cycle (Ravanel et al., 2004; Rébeillé et al., 2007). De novo Met biosynthesis in plants is known to occur in plastids, and a critical step in the formation of this amino acid is the methylation of homo-Cys, which is catalyzed by a plastid-localized Met synthase (Ravanel et al., 2004). The C1 unit transferred to homo-Cys is donated by 5-CH_3-THF to form Met (Rébeillé et al., 2006; Fig. 1). Because Met synthase cannot efficiently utilize monoglutamate forms of 5-CH_3-THF (Ravanel et al., 2004), a substantial amount of the folate pool in the mutant (Fig. 9) cannot be used for Met biosynthesis. Indeed, metabolic profiling showed that endogenous Met levels were lower in *atdfb* seedlings compared with the wild type (Fig. 10). A large percentage of the Met flux goes to AdoMet synthesis, which is involved in methylation reactions for the metabolism of nucleic acids, proteins, lipids, and various secondary metabolites. Thus, the lower levels of Met in *atdfb* resulting from reduced FPGS activity could explain the alterations in a large number of cellular metabolites (Supplemental Tables S2 and S3) and the cytoskeletal, cell division, and cell expansion defects in roots, as these processes are highly dependent on products of cellular methylation reactions. This notion is supported by the observation that exogenous application of Met caused a partial restoration of root growth in *atdfb* (Supplemental Fig. S6).

The reduced levels of adenine and guanosine that may result from inadequate 10-CHO-THF polyglutamates could also contribute to defective *atdfb* root growth, given their important role as building blocks of DNA and as major energy donors in numerous metabolic reactions of the cell (Zrenner et al., 2006). However, only guanosine caused a promotion in root length of *atdfb*. It is possible that certain metabolites that are applied exogenously, including Met and guanosine, which were only able to partially restore root growth in the mutant, cannot reach a population of cells such as the QC, where they are needed most. Alternatively, the applied compounds could be rapidly metabolized into forms that the cell cannot utilize for restoring complete biochemical function. Moreover, a combination of depleted levels of other metabolites combined with the toxic accumulation of others (e.g. adenosine) likely defines the overall root defects of *atdfb*. A more targeted analysis of metabolites within a defined population of cells, particularly those that participate in C1 transfer reactions such as AdoMet and homo-Cys, will be needed to fully understand how changes in folate glutamylation impact root development.

In conclusion, we provide genetic evidence that AtDFB plays a pivotal role in postembryonic primary root development in Arabidopsis. Consequences of mutating the *AtDFB* gene include the accumulation of monoglutamylated folates, broad alterations to seedling metabolite levels, and various root cell defects that could be attributed in part to the loss of QC identity. Taken together, our results indicate that although redundancy in FPGS function is operating for certain plant developmental processes (Mehrshahi et al., 2010), a single FPGS isoform can play a critical role in the metabolism of a specific cell population to influence root growth within a defined window of development.

MATERIALS AND METHODS

Isolation of *atdfb* Mutants

atdfb-1 (originally designated as *drh2* for *defective root hair2*; Supplemental Fig. S1) was identified through a forward genetic screen for mutants with abnormal root hairs (Yoo et al., 2008). Screening was done on a population of Arabidopsis (*Arabidopsis thaliana*) ecotype Columbia (Col-0) T-DNA-mutagenized seed stock (CS31100) from the Arabidopsis Biological Resource Center (ABRC). *atdfb-1* was back-crossed to Col-0 at least two times to remove extraneous mutations. The location of T-DNA in the mutant was determined by thermal asymmetric interlaced PCR (Liu et al., 1995). Two additional lines with T-DNA insertions at the *AtDFB* locus (SALK_015472 and SAIL_556_G08) were obtained from the ABRC (Alonso et al., 2003). These lines were renamed *atdfb-2* and *atdfb-3*, respectively, after confirming the T-DNA insertion site and observing that the root phenotypes of these additional T-DNA lines were similar to *atdfb-1* (Fig. 3). Mutants to the *AtDFC* (SALK_008883) and *AtDFD* (SAIL_151_E09) genes were also obtained from the ABRC, and genotyping of these lines was essentially as described above (Supplemental Fig. S3).

Phenotypic Characterization of *atdfb*

For phenotypic analyses, seeds of the wild type (Col-0) and mutants were surface sterilized with 95% (v/v) ethanol and 20% (v/v) bleach and washed extensively with sterile water before germinating these seeds on solid half-strength Murashige and Skoog medium (pH 5.7) containing 1% (w/v) Suc, phytagar (0.5%–1%), and vitamins pyridoxine-HCl, nicotinic acid (0.5 mg mL^{-1}), and thiamine (1 mg mL^{-1}). Plates were incubated vertically in a controlled-environment chamber at 120 to 140 μmol photons m^{-2} s^{-1}, 14 h of

light at 22°C, and 10 h of dark at 19°C. Digital photographs of primary roots and root hairs at various stages of seedling development were acquired, and their lengths were measured using ImageJ.

For 5-CHO-THF [(6*S*)-5-formyl-5,6,7,8-tetrahydrofolic acid, calcium salt; natural calcium folinate; Schircks Laboratories], Met, adenine, and guanosine (Sigma) supplementation experiments, stock solutions were applied to the growth medium to achieve the desired working concentration. Briefly, adenine and guanosine were dissolved in 1 mL of deionized water with two to three drops of 1 M KOH. From this initial solution, a 10 mM stock solution was made by bringing the final volume to 10 mL with deionized water. For 5-CHO-THF and Met, a stock solution of 10 mM was made using deionized water. Seeds were either planted directly or seedlings were transplanted on the growth medium and root growth assays were performed as described earlier.

Transcript Analysis and Whole Mount in Situ Hybridization

Total RNA was isolated using an RNeasy Mini Kit (Qiagen) and reverse transcribed using a First-Strand cDNA Kit with oligo(dT)$_{20}$ and SuperScript III reverse transcriptase (Invitrogen). For semiquantitative PCR, first-strand cDNA was amplified with Platinum Taq High Fidelity (Invitrogen). Cycling parameters were 94°C for 10 s, 60°C for 15 s, and 72°C for 50 s.

For quantitative two-step RT-PCR of *AtDFB* and *AGL42*, 1 μg of total RNA from the wild type and *atdfb-1* was reverse transcribed to first-strand cDNA with the Qiagen cDNA Synthesis Kit (Qiagen). First-strand cDNA was used as a template for quantitative PCR using gene-specific primers. Arabidopsis *eukaryotic initiation factor4A-2* (*EIF4A-2*) served as a control for constitutive gene expression in plants. Primers used are shown in Supplemental Table S4. Relative expression levels using the formula for threshold cycle ($2^{-\Delta Ct}$) were calculated according to Ramakers et al. (2003). Expression levels of *AtDFB* were calculated based on the relative level of *EIF4A-2* expression in each sample. Values are means of three biological replicates with three technical replicates for each.

Four-day-old seedlings were processed for in situ hybridization essentially as described by Hejátko et al. (2006) using *AtDFB*-specific probes (Supplemental Table S4). Roots were examined with a Nikon Microphot FX compound microscope, and images were acquired using a Nikon DXM 1200 camera running on ACT-1 software (Nikon Instruments).

Cell Biological Studies of Roots

The *atdfb-1* mutants were transformed with a GFP construct that binds to F-actin (GFP-ABD2-GFP; Wang et al., 2008) and our independently generated *DR5:GFPm*. The *DR5* auxin-responsive element was a gift from Dr. Tom Guilfoyle (University of Missouri; Ulmasov et al., 1997). Seeds of the wild type and *atdfb-1* expressing GFP-ABD2-GFP and *DR5:GFPm* were germinated on 64- × 48-mm cover glasses coated with growth medium as described by Wang et al. (2008). Plates were incubated vertically for 4 to 8 d at 21°C with a 14-h photoperiod. Primary roots of wild-type and *atdfb-1* seedlings expressing the reporters were imaged with a Leica TCS SP2 AOBS confocal laser-scanning microscope. GFP was excited using the 488-nm line of the argon laser, and emission was detected at 510 nm. QC organization was evaluated in confocal median longitudinal sections of roots stained for 5 min with 10 μM propidium iodide. In a parallel set of experiments, mature embryos from the wild type and *atdfb-1* were dissected from seeds imbibed for 24 h in water and the QC was imaged in aniline blue-stained embryos as described by Bougourd et al. (2000).

For evaluating mitosis, 4-d-old seedlings were fixed in 1× PME (50 mM PIPES, 2 mM $MgCl_2$, and 10 mM EGTA, pH 7.0) buffer containing 2% formaldehyde and 0.5% glutaraldehyde as described previously (Heslop-Harrison, 1998). After repeated washing with PMET (PME + 0.1% Triton X-100), fixed seedlings were digested with an enzyme solution containing 100 mg mL^{-1} Cellulase (Sigma) dissolved in 20 mL of PMET along with 1.5 g of mannitol at room temperature for 20 min. After repeated rinsing in PME, roots were stained with DAPI (1:10,000 stock dilution) for 2 h. DAPI was excited using a 405-nm blue diode laser and emission was detected at 458 nm using a confocal microscope. The number of mitotic cells from the apical 100 μm of the root apex was counted from projected images of 26 confocal optical sections taken at 1-μm intervals.

To visualize amyloplasts, 7-d-old seedlings were fixed in 4% formaldehyde and stained with potassium iodide (Lugol's solution) as described by Willemsen et al. (1998).

Folate Analysis

Shoots and roots from 15-d-old wild-type and mutant seedlings were analyzed for folates from 1 g of total tissue by HPLC as described previously (Goyer et al., 2005; Orsomando et al., 2005) with slight modifications: half of the folate extract was deglutamylated using a purified mixture of Arabidopsis recombinant γ-glutamyl hydrolase isoforms 1 and 2 (Orsomando et al., 2005; 0.1 mg of each protein per g of tissue, with a 2-h incubation time). The rest of the extract was used for profiling folate polyglutamylation. Purified extracts were separated by HPLC using an Atlantis dC18 column (150 × 4.6 mm, 5 μm; Waters) and analyzed by a four-channel electrochemical detector (CoulArray model 5600A; ESA Inc.) with potentials set at 100, 200, 300, and 400 mV. Detector response was calibrated using THF, 5-CH_3-THF, 5-CHO-THF, and 5,10-CH_2-THF standards (Schircks Laboratories).

Metabolite Analyses by GC-MS

Metabolite analyses were carried out using a GC-MS-based method modified from Broeckling et al. (2005). Briefly, 7-d-old seedlings were lyophilized, homogenized, vortexed, and then incubated for 45 min at 50°C in glass vials after adding chloroform containing 10 μg mL^{-1} docosanol (internal standard). After samples equilibrated to room temperature, 1.5 mL of HPLC-grade water containing 25 μg mL^{-1} ribitol was added and samples were incubated for another 45 min at 50°C. The biphasic solvent mixture was then centrifuged at 2,900*g* for 30 min. One milliliter of each layer was transferred to individual autosampler vials and dried under nitrogen for the nonpolar/chloroform aliquots and in a vacuum centrifuge for polar/aqueous aliquots. The dried nonpolar extracts were resuspended in chloroform and trans-esterified by adding HCl in methanol. Following trans-esterification for 4 h at 50°C, samples were evaporated under nitrogen, resuspended in pyridine, and derivatized using *N*-methyl-*N*-trimethylsilyltrifluoroacetamide + 1% trimethyl chlorosilane (Pierce Biotechnology) for 1 h at 50°C. The samples were equilibrated to room temperature, transferred to glass inserts, and analyzed by GC-MS.

The dried polar extracts were methoximated in pyridine with methoxyamine-HCl, briefly sonicated, and incubated for 1 h at 50°C. Metabolites were then derivatized with *N*-methyl-*N*-trimethylsilyltrifluoroacetamide + 1% trimethyl chlorosilane for 1 h at 50°C and analyzed by GC-MS. The GC system used was an Agilent 6890 coupled to a 5973 MSD quadrupole mass spectrometer scanning from mass-to-charge ratio 50 to 650. Acquired mass spectra were deconvoluted using AMDIS software, and metabolite identifications were achieved by mass spectral matching to the Noble Foundation's in-house electron ionization-MS spectral library of authentic compounds, the publicly available GOLM library (http://csbdb.mpimp-golm.mpg.de/csbdb/dbma/msri.html), and the NIST08 library. Peak selection and alignment were performed using MET-IDEA software (Broeckling et al., 2006). The area of each peak was normalized against the area of the internal standard, and absolute quantification for selected metabolites was achieved using authentic standard calibration curves.

Sequence data from this article can be found in the Arabidopsis Genome Initiative or GenBank/EMBL databases under the following accession numbers: for AtDFB, NP_196217 and At5g05980.

Supplemental Data

The following materials are available in the online version of this article.

Supplemental Figure S1. *drh2* (*atdfb-1*) has short and wavy root hairs.

Supplemental Figure S2. *AtDFB* knockouts have no obvious defects in shoot development when compared with the wild type.

Supplemental Figure S3. Identification of mutants to *AtDFC* and *AtDFD*.

Supplemental Figure S4. *AtDFB* is more strongly expressed in roots compared with *AtDFC* and *AtDFD*.

Supplemental Figure S5. 5-CHO-THF rescues the cell division and root hair phenotypes of *atdfb*.

Supplemental Figure S6. Exogenous Met and guanosine promote root growth in *atdfb* seedlings.

Supplemental Table S1. Total folate content in shoots and roots of 15-d-old Arabidopsis seedlings.

Supplemental Table S2. Polar metabolites from 7-d-old wild-type and *atdfb-1* seedlings.

Supplemental Table S3. Nonpolar metabolites from 7-d-old wild-type and *atdfb-1* seedlings.

Supplemental Table S4. Primer sequences used for genotyping and gene expression analysis.

ACKNOWLEDGMENTS

We thank Drs. Andrew Hanson (University of Florida), Richard Dixon, and Rao Uppalapati (Noble Foundation) for critical review of the manuscript. We also thank J. Alan Sparks and Dr. Tui Ray (Noble Foundation) for technical assistance.

Received October 26, 2010; accepted January 13, 2011; published January 13, 2011.

LITERATURE CITED

Alonso JM, Stepanova AN, Leisse TJ, Kim CJ, Chen H, Shinn P, Stevenson DK, Zimmerman J, Barajas P, Cheuk R, et al (2003) Genome-wide insertional mutagenesis of *Arabidopsis thaliana*. Science **301:** 653–657

Appling DR (1991) Compartmentation of folate-mediated one-carbon metabolism in eukaryotes. FASEB J **5:** 2645–2651

Beck M, Komis G, Müller J, Menzel D, Samaj J (2010) *Arabidopsis* homologs of nucleus- and phragmoplast-localized kinase 2 and 3 and mitogen-activated protein kinase 4 are essential for microtubule organization. Plant Cell **22:** 755–771

Bedhomme M, Hoffmann M, McCarthy EA, Gambonnet B, Moran RG, Rébeillé F, Ravanel S (2005) Folate metabolism in plants: an Arabidopsis homolog of the mammalian mitochondrial folate transporter mediates folate import into chloroplasts. J Biol Chem **280:** 34823–34831

Benfey PN, Bennett M, Schiefelbein J (2010) Getting to the root of plant biology: impact of the Arabidopsis genome sequence on root research. Plant J **61:** 992–1000

Benková E, Hejátko J (2009) Hormone interactions at the root apical meristem. Plant Mol Biol **69:** 383–396

Bernal AJ, Yoo CM, Mutwil M, Jensen JK, Hou G, Blaukopf C, Sørensen I, Blancaflor EB, Scheller HV, Willats WG (2008) Functional analysis of the cellulose synthase-like genes CSLD1, CSLD2, and CSLD4 in tip-growing Arabidopsis cells. Plant Physiol **148:** 1238–1253

Besson V, Neuburger M, Rébeillé F, Douce R (1995) Evidence for three serine hydroxymethyltransferases in green leaf cells: purification and characterization of the mitochondrial and chloroplastic isoforms. Plant Physiol Biochem **33:** 665–673

Blancaflor EB, Wang YS, Motes CM (2006) Organization and function of the actin cytoskeleton in developing root cells. Int Rev Cytol **252:** 219–264

Bougourd S, Marrison J, Haseloff J (2000) Technical advance: an aniline blue staining procedure for confocal microscopy and 3D imaging of normal and perturbed cellular phenotypes in mature Arabidopsis embryos. Plant J **24:** 543–550

Broeckling CD, Huhman DV, Farag MA, Smith JT, May GD, Mendes P, Dixon RA, Sumner LW (2005) Metabolic profiling of *Medicago truncatula* cell cultures reveals the effects of biotic and abiotic elicitors on metabolism. J Exp Bot **56:** 323–336

Broeckling CD, Reddy IR, Duran AL, Zhao X, Sumner LW (2006) MET-IDEA: data extraction tool for mass spectrometry-based metabolomics. Anal Chem **78:** 4334–4341

Chen H, Xiong L (2005) Pyridoxine is required for post-embryonic root development and tolerance to osmotic and oxidative stresses. Plant J **44:** 396–408

Chen H, Xiong L (2009) The short-rooted vitamin B6-deficient mutant pdx1 has impaired local auxin biosynthesis. Planta **229:** 1303–1310

Cherest H, Thomas D, Surdin-Kerjan Y (2000) Polyglutamylation of folate coenzymes is necessary for methionine biosynthesis and maintenance of intact mitochondrial genome in *Saccharomyces cerevisiae*. J Biol Chem **275:** 14056–14063

Collakova E, Goyer A, Naponelli V, Krassovskaya I, Gregory JF III, Hanson AD, Shachar-Hill Y (2008) *Arabidopsis* 10-formyl tetrahydrofolate deformylases are essential for photorespiration. Plant Cell **20:** 1818–1832

Cossins EA (2000) The fascinating world of folate and one-carbon metabolism. Can J Bot **78:** 691–708

Cossins EA, Chen L (1997) Folates and one-carbon metabolism in plants and fungi. Phytochemistry **45:** 437–452

Cox K, Robertson D, Fites R (1999) Mapping and expression of a bifunctional thymidylate synthase, dihydrofolate reductase gene from maize. Plant Mol Biol **41:** 733–739

Forde BG, Walch-Liu PIA (2009) Nitrate and glutamate as environmental cues for behavioural responses in plant roots. Plant Cell Environ **32:** 682–693

Goyer A, Collakova E, Díaz de la Garza R, Quinlivan EP, Williamson J, Gregory JF III, Shachar-Hill Y, Hanson AD (2005) 5-Formyltetrahydrofolate is an inhibitory but well tolerated metabolite in Arabidopsis leaves. J Biol Chem **280:** 26137–26142

Hanson AD, Gage DA, Shachar-Hill Y (2000) Plant one-carbon metabolism and its engineering. Trends Plant Sci **5:** 206–213

Hanson AD, Gregory JF III (2002) Synthesis and turnover of folates in plants. Curr Opin Plant Biol **5:** 244–249

Hanson AD, Roje S (2001) One-carbon metabolism in higher plants. Annu Rev Plant Physiol Plant Mol Biol **52:** 119–137

Hejátko J, Blilou I, Brewer PB, Friml J, Scheres B, Benková E (2006) In situ hybridization technique for mRNA detection in whole mount Arabidopsis samples. Nat Protoc **1:** 1939–1946

Heslop-Harrison JS (1998) Cytogenetic analysis of Arabidopsis. Methods Mol Biol **82:** 119–127

Ishikawa T, Machida C, Yoshioka Y, Kitano H, Machida Y (2003) The GLOBULAR ARREST1 gene, which is involved in the biosynthesis of folates, is essential for embryogenesis in *Arabidopsis thaliana*. Plant J **33:** 235–244

Iyer-Pascuzzi A, Simpson J, Herrera-Estrella L, Benfey PN (2009) Functional genomics of root growth and development in Arabidopsis. Curr Opin Plant Biol **12:** 165–171

Jabrin S, Ravanel S, Gambonnet B, Douce R, Rébeillé F (2003) One-carbon metabolism in plants: regulation of tetrahydrofolate synthesis during germination and seedling development. Plant Physiol **131:** 1431–1439

Klaus SM, Kunji ER, Bozzo GG, Noiriel A, de la Garza RD, Basset GJ, Ravanel S, Rébeillé F, Gregory JF III, Hanson AD (2005) Higher plant plastids and cyanobacteria have folate carriers related to those of trypanosomatids. J Biol Chem **280:** 38457–38463

Lin BF, Huang RF, Shane B (1993) Regulation of folate and one-carbon metabolism in mammalian cells. III. Role of mitochondrial folylpoly-gamma-glutamate synthetase. J Biol Chem **268:** 21674–21679

Liu YG, Mitsukawa N, Oosumi T, Whittier RF (1995) Efficient isolation and mapping of *Arabidopsis thaliana* T-DNA insert junctions by thermal asymmetric interlaced PCR. Plant J **8:** 457–463

Loizeau K, De Brouwer V, Gambonnet B, Yu A, Renou JP, Van Der Straeten D, Lambert WE, Rébeillé F, Ravanel S (2008) A genome-wide and metabolic analysis determined the adaptive response of Arabidopsis cells to folate depletion induced by methotrexate. Plant Physiol **148:** 2083–2095

Loizeau K, Gambonnet B, Zhang GF, Curien G, Jabrin S, Van Der Straeten D, Lambert WE, Rébeillé F, Ravanel S (2007) Regulation of one-carbon metabolism in Arabidopsis: the N-terminal regulatory domain of cystathionine gamma-synthase is cleaved in response to folate starvation. Plant Physiol **145:** 491–503

Lucas M, Swarup R, Paponov IA, Swarup K, Casimiro I, Lake D, Peret B, Zappala S, Mairhofer S, Whitworth M, et al (2011) SHORT-ROOT regulates primary, lateral, and adventitious root development in Arabidopsis. Plant Physiol **155:** 384–398

Mehrshahi P, Gonzalez-Jorge S, Akhtar TA, Ward JL, Santoyo-Castelazo A, Marcus SE, Lara-Núñez A, Ravanel S, Hawkins ND, Beale MH, et al (2010) Functional analysis of folate polyglutamylation and its essential role in plant metabolism and development. Plant J **64:** 267–279

Nawy T, Lee JY, Colinas J, Wang JY, Thongrod SC, Malamy JE, Birnbaum K, Benfey PN (2005) Transcriptional profile of the *Arabidopsis* root quiescent center. Plant Cell **17:** 1908–1925

Orsomando G, de la Garza RD, Green BJ, Peng M, Rea PA, Ryan TJ, Gregory JF III, Hanson AD (2005) Plant gamma-glutamyl hydrolases and folate polyglutamates: characterization, compartmentation, and co-occurrence in vacuoles. J Biol Chem **280:** 28877–28884

Ottenschläger I, Wolff P, Wolverton C, Bhalerao RP, Sandberg G,

Ishikawa H, Evans M, Palme K (2003) Gravity-regulated differential auxin transport from columella to lateral root cap cells. Proc Natl Acad Sci USA **100:** 2987–2991

Overvoorde P, Fukaki H, Beeckman T (2010) Auxin control of root development. Cold Spring Harb Perspect Biol **2:** a001537

Qi H, Atkinson I, Xiao S, Choi YJ, Tobimatsu T, Shane B (1999) Folylpolygamma-glutamate synthetase: generation of isozymes and the role in one carbon metabolism and antifolate cytotoxicity. Adv Enzyme Regul **39:** 263–273

Quinlivan EP, Hanson AD, Gregory JF (2006) The analysis of folate and its metabolic precursors in biological samples. Anal Biochem **348:** 163–184

Raichaudhuri A, Peng M, Naponelli V, Chen S, Sánchez-Fernández R, Gu H, Gregory JF III, Hanson AD, Rea PA (2009) Plant vacuolar ATP-binding cassette transporters that translocate folates and antifolates in vitro and contribute to antifolate tolerance in vivo. J Biol Chem **284:** 8449–8460

Ramakers C, Ruijter JM, Deprez RHL, Moorman AFM (2003) Assumption-free analysis of quantitative real-time polymerase chain reaction (PCR) data. Neurosci Lett **339:** 62–66

Ravanel S, Block MA, Rippert P, Jabrin S, Curien G, Rébeillé F, Douce R (2004) Methionine metabolism in plants: chloroplasts are autonomous for de novo methionine synthesis and can import S-adenosylmethionine from the cytosol. J Biol Chem **279:** 22548–22557

Ravanel S, Cherest H, Jabrin S, Grunwald D, Surdin-Kerjan Y, Douce R, Rébeillé F (2001) Tetrahydrofolate biosynthesis in plants: molecular and functional characterization of dihydrofolate synthetase and three isoforms of folylpolyglutamate synthetase in *Arabidopsis thaliana*. Proc Natl Acad Sci USA **98:** 15360–15365

Rébeillé F, Ravanel S, Jabrin S, Douce R, Storozhenko S, Van Der Straeten D (2006) Folates in plants: biosynthesis, distribution, and enhancement. Physiol Plant **126:** 330–342

Rébeillé F, Ravanel S, Marquet A, Mendel RR, Webb ME, Smith AG, Warren MJ (2007) Roles of vitamins B5, B8, B9, B12 and molybdenum cofactor at cellular and organismal levels. Nat Prod Rep **24:** 949–962

Roje S, Chan SY, Kaplan F, Raymond RK, Horne DW, Appling DR, Hanson AD (2002) Metabolic engineering in yeast demonstrates that S-adenosylmethionine controls flux through the methylenetetrahydrofolate reductase reaction in vivo. J Biol Chem **277:** 4056–4061

Sabatini S, Beis D, Wolkenfelt H, Murfett J, Guilfoyle T, Malamy J, Benfey P, Leyser O, Bechtold N, Weisbeek P, et al (1999) An auxin-dependent distal organizer of pattern and polarity in the Arabidopsis root. Cell **99:** 463–472

Sabatini S, Heidstra R, Wildwater M, Scheres B (2003) SCARECROW is involved in positioning the stem cell niche in the Arabidopsis root meristem. Genes Dev **17:** 354–358

Sahr T, Ravanel S, Rébeillé F (2005) Tetrahydrofolate biosynthesis and distribution in higher plants. Biochem Soc Trans **33:** 758–762

Stover P, Schirch V (1993) The metabolic role of leucovorin. Trends Biochem Sci **18:** 102–106

Ulmasov T, Murfett J, Hagen G, Guilfoyle TJ (1997) Aux/IAA proteins repress expression of reporter genes containing natural and highly active synthetic auxin response elements. Plant Cell **9:** 1963–1971

van den Berg C, Willemsen V, Hendriks G, Weisbeek P, Scheres B (1997) Short-range control of cell differentiation in the Arabidopsis root meristem. Nature **390:** 287–289

Wagner S, Bernhardt A, Leuendorf JE, Drewke C, Lytovchenko A, Mujahed N, Gurgui C, Frommer WB, Leistner E, Fernie AR, et al (2006) Analysis of the *Arabidopsis rsr4-1/pdx1-3* mutant reveals the critical function of the PDX1 protein family in metabolism, development, and vitamin B6 biosynthesis. Plant Cell **18:** 1722–1735

Wang YS, Yoo CM, Blancaflor EB (2008) Improved imaging of actin filaments in transgenic Arabidopsis plants expressing a green fluorescent protein fusion to the C- and N-termini of the fimbrin actin-binding domain 2. New Phytol **177:** 525–536

Willemsen V, Wolkenfelt H, de Vrieze G, Weisbeek P, Scheres B (1998) The HOBBIT gene is required for formation of the root meristem in the Arabidopsis embryo. Development **125:** 521–531

Yoo CM, Wen J, Motes CM, Sparks JA, Blancaflor EB (2008) A class I ADP-ribosylation factor GTPase-activating protein is critical for maintaining directional root hair growth in Arabidopsis. Plant Physiol **147:** 1659–1674

Zhang Y, Sun K, Sandoval FJ, Santiago K, Roje S (2010) One-carbon metabolism in plants: characterization of a plastid serine hydroxymethyltransferase. Biochem J **430:** 97–105

Zimmermann P, Hirsch-Hoffmann M, Hennig L, Gruissem W (2004) GENEVESTIGATOR: Arabidopsis microarray database and analysis toolbox. Plant Physiol **136:** 2621–2632

Zrenner R, Stitt M, Sonnewald U, Boldt R (2006) Pyrimidine and purine biosynthesis and degradation in plants. Annu Rev Plant Biol **57:** 805–836